Peertechz


CHEMISTRY GROUP

ARCHIVE OF Biochemistry

DOI: https://dx.doi.org/10.17352/ab

Research Article

# Identifying potential regulatory interactions of peroxiredoxin PRXQ

**Jason Kreinces***

New York Medical College, Valhalla, New York, USA

**Received:** 23 December, 2020
**Accepted:** 28 December, 2020
**Published:** 30 December, 2020

***Corresponding author:** Jason Kreinces, New York Medical College, Valhalla, New York, USA,
E-mail: jkreinces14@yahoo.com

**Keywords:** Peroxiredoxin; Glutaredoxin; Thioredoxin; Reactive oxygen species; Oxidative damage; Antioxidant

https://www.peertechz.com

Check for updates

## Abstract

Peroxiredoxins (Prxs) are cysteine-based peroxide-reducing enzymes that have been extensively studied over the past two decades. The reduction of the Prx disulfide form is dependent on electron donating enzymes to shift the Prx back into a catalytically active state. However, this reaction is poorly understood and reductant enzymes for this reaction to reduce the Prx disulfide bond have received little attention. Prxs from the bacterium *Xanthomonas campestris* (XcPrxQ) were used to assess how reductants affect Prx turnover by identifying potential electron transfer interactions between Prxs and reductants, Glutaredoxins (Grxs) and Thioredoxins (Trxs). To examine potential interactions between PrxQ and reducing proteins, we used PrxQ, Grx, and Trx mutants to determine the effect of specific cysteines in each of the proteins. Mutant and wildtype proteins were expressed in *E. coli* and purified using anion-exchange and gel filtration chromatography and purity was verified by SDS-PAGE. The results clarified the role of the two cysteines in PrxQ, C48 and C84, which are thought to participate in the reduction reaction of hydrogen peroxide. They also show Trx and Grx proteins from the same bacterium are possible reductants for Prx turnover, as reactions with PrxQ have produced complex formation at a larger molecular weight, suggesting the reductant binding to PrxQ and reducing its disulfide bond. This study is significant because it reveals potential binding interactions between reductants and Prxs that regulate Prx turnover into a catalytically active state, allowing the enzyme to break down peroxide and prevent oxidative damage, as well as highlighting Trxs in bacteria as a potential drug target due to their regulation of hydrogen peroxide levels in pathogenic strains.

## Introduction

Reactive Oxygen Species (ROS) serve as key signaling molecules in many beneficial signaling cascades. Hydrogen peroxide is a ROS that can be a by-product of enzymatic reactions involved in metabolism and other biological systems or produced by NADPH oxidases (NOXs). The role of NOX enzymes has been demonstrated in many important signaling pathways crucial for human health, including responses triggered by cytokines, growth factors, and toll-like receptors of the innate immune system [1]. Hydrogen peroxide is a common free radical utilized by the human immune system to help kill infectious bacteria and other organisms [2]. It has also been found to have surprising growth promoting roles, as it has been seen that it mimics the stimulatory effects that insulin causes on glucose uptake and promotes lipid and protein production [1,3].

While small, localized concentration changes in ROS have beneficial functions as signaling molecules, at high levels, ROS, such as peroxide, are major contributors to oxidative stress, which can damage the structures of DNA, RNA, proteins, and lipids [4]. Oxidative damage of these structures has been extensively studied and well-known outcomes of oxidative damage include cell death and pathological progression of various diseases, including cancer [4]. Oxidative damage is also capable of bacterial destruction. It is important for both humans and prokaryotes to manage endogenous ROS levels to prevent their harmful effects. For this reason, organisms utilize a variety of antioxidant defense mechanisms including the proteins, peroxiredoxins (Prxs).

Prxs are abundant cysteine-based peroxidases found in nearly all organisms, which break down hydrogen peroxide, alkyl hydroperoxides, and peroxynitrite [5]. These proteins are important for regulating intracellular hydrogen peroxide levels and key signaling pathways where hydrogen peroxide is used as a secondary signaling molecule. Prxs comprise a crucial part of the bacterial defense against toxic free radicals, including peroxides [6]. These enzymes use reactive cysteine thiols via electron transfer to reduce these potentially cell-damaging free radicals. These proteins are important for preventing oxidative stress from occurring within the organism induced by both exogenous peroxides and endogenous peroxides



**Citation:** Kreinces J (2020) Identifying potential regulatory interactions of peroxiredoxin PRXQ. Arch Biochem 2(1): 010-019. DOI: https://dx.doi.org/10.17352/ab.000003

produced by metabolic processes.[6] In addition to bacterium utilizing this system for maintain homeostatic defense against ROS, Prxs have also been implicated in accentuating bacterial pathogenicity, further promoting bacterial survival [7].

To understand the functional and structural characteristics of Prx enzymes, monomeric Prxs from the bacterium *Xanthomonas campestris* (XcPrxQ) have been used as a model to further explore Prx reactivity and structure [5,8,9]. XcPrxQ enzymes are cysteine-based Prxs, which are characterized by two cysteine residues in its active site (Figure 1). The basic protein is a monomer, and the catalytic disulfide bond is formed between the two cysteine (Cys) residues upon reduction of the peroxide (Figure 2). As described previously by Reeves, et al. [10]. Prxs utilize the active site Cys residue, known as the peroxidatic Cys ($C_p$), to react with a peroxide substrate, generating a Cyssulfenic acid (Cys-SOH) on the protein residue.

The second Cys, known as the resolving Cys ($C_R$), reacts with the sulfenic acid to release water and forms a disulfide bond to protect the protein from further oxidation [10]. The catalytic cycle is completed once the disulfide bond is reduced, freeing up the thiol groups for further breakdown of peroxide molecules (Figure 2). In *XcPrxQ*, Cys 48 has been identified as the peroxidatic Cys while Cys 84 has the role of the resolving Cys [8]. Using two mutant versions of the protein, *Xc* PrxQ C48S and *Xc PrxQ* C84S, we are able to assess the reactivity of each residue with peroxide as well as potential reductants. Each of these residues is replaced with a catalytically inactive serine (Ser) residue, to measure the chemical reactivity kinetics of each Cys residue.

While studies have been performed on the hydrogen peroxide reduction reaction, much less attention has been given to potential electron donors required to sustain catalytic turnover. This study was designed to learn more about Prx regulation and Prx turnover by examining potential electron transfer interactions of PrxQ with two target reductants, Tthioredoxin (Trx) and Glutaredoxin (Grx), from the same bacterium, which may promote Prx turnover and allow heightened reduction of peroxides.

## Materials and methods

### Mutagenesis of PrxQ, Trx, and Grx from the bacterium Xanthomonas campestris

The two mutants of XcPrxQ, C48S and C84S, were previously generated using a QuikChange mutagenesis protocol [8]. In each mutant, one Cys residue is mutated to a Ser to prevent a disulfide formation between the two-active site Cys residues, and that Ser cannot react with DTNB in the following assays (Figure 3). Wild-type and mutant constructs of XcTrx (C33S and C36S) and of XcGrx (C24S and C27S) were synthesized in vitro by GenScript (Jiangsu Province, China). These genes were provided as clones in the pUC57 vector.

### Construction of Grx expression constructs and expression of Grx protein

The pET-28a expression vector was used for subcloning.

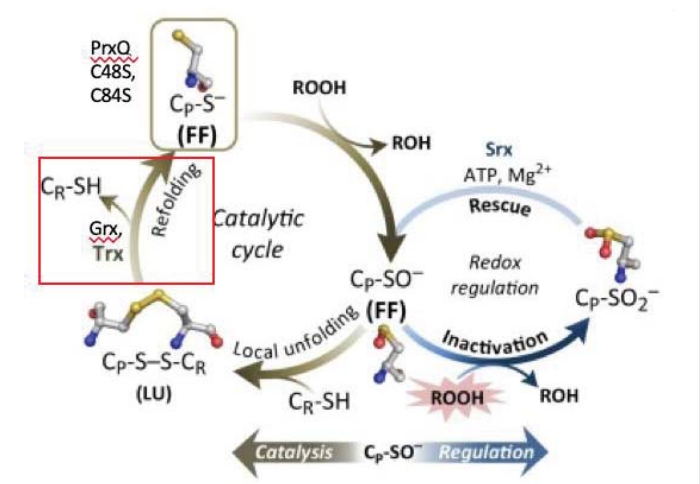


**Figure 1:** Catalytic Cycle of Prx. The red box highlights the primary focus of the study; potential reductants to reduce the Prx disulfide bond. In order to test this, PrxQ is reacted with DTNB to mimic the disulfide substrate seen in the final step of catalysis. This reaction forms the PrxQ-NTB conjugates and can be tracked by the release of a free NTB molecule which makes the solution yellow and has a strong absorbance signal at 412 nm. $C_p$ is the peroxidatic Cys, or the Cys that attacks hydrogen peroxide. $C_R$ is the resolving Cys, or the residue that forms the disulfide bond with the $C_p$ to complete the catalytic cycle.

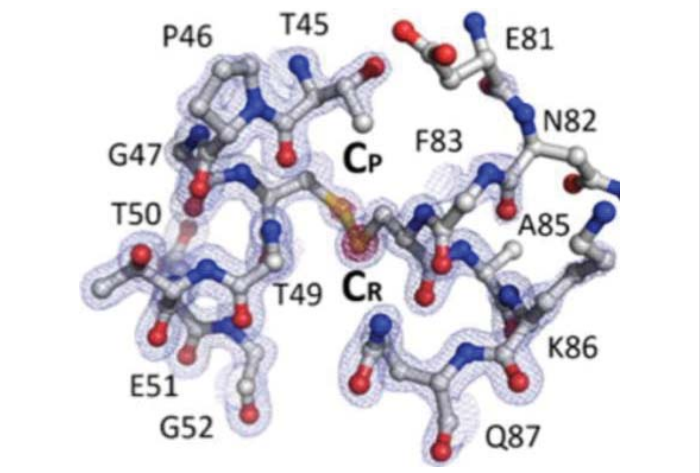


**Figure 2:** Crystal structure of PrxQ. The two reactive cysteines are labeled $C_p$ and $C_R$. The cysteines are in a disulfide bond following catalysis of hydrogen peroxide, indicating the protein is in its inactive form as both thiols are unreactive in the disulfide linkage.

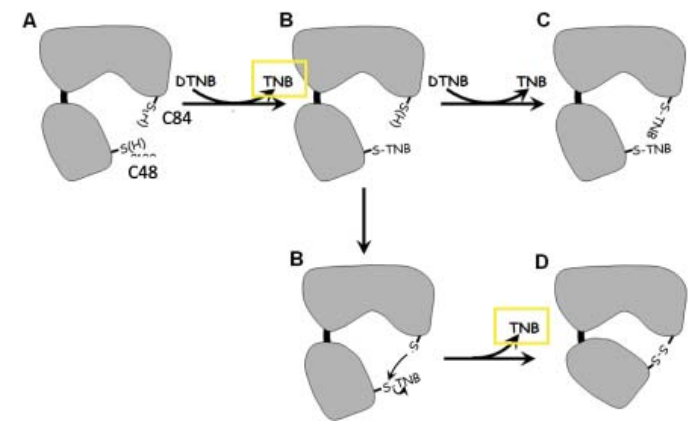


**Figure 3:** Potential reaction pathways of PrxQ thiols with DTNB. The reaction can proceed in two distinct ways: both thiol groups can react with DTNB or the wild type will form a disulfide bond to displace the TNB. Thus, this is why one of the cysteine residues is mutated in order to obtain single PrxQ-NTB conjugates.



**Citation:** Kreinces J (2020) Identifying potential regulatory interactions of peroxiredoxin PRXQ. Arch Biochem 2(1): 010-019. DOI: https://dx.doi.org/10.17352/ab.000003

The clones were in the pUC57 vector, which has *NcoI* and *HindIII* restriction sites flanking the insert. The pUC57 vector with inserted genes as well as the expression vector pET-28A was incubated with *Nco*I and *Hin*dIII for 30 min. The fragments from the digestion were purified from agarose gels. DNA fragments were ligated using T4 DNA ligase. Successful ligation was confirmed by gel electrophoresis.

Ligation mixtures were transformed into XL1-Blue *E. coli* cells. The ligation mixture containing the plasmid DNA was added to the *E. coli* cells. Cells were then mixed with 800 µl of LB media and incubated in a shaking incubator (200 rpm) at 37ºC for 60 minutes. After shaking, the cells were centrifuged at 14,000 rpm (diameter = 11.96 cm) for 20 seconds, and all but about 200 µL of the supernatant was discarded. Cells were resuspended and spread onto LB media plates and incubated overnight at 37°C. DNA-mini preparation of these cultures was done to isolate the DNA plasmid containing the Grx gene using the QIAprep kit from QIAGEN. Restriction digestion was performed to confirm the correct insert was present in the plasmid and analyzed by gel electrophoresis.

The pure plasmid DNA was then transformed into the BL21 Gold DE3 *E. coli* expression strain. Transformed bacterial cells were inoculated in auto-induction media and grown overnight to allow expression of the protein. To check for successful expression of the Grx mutant proteins, samples of the cells were run on SDS-PAGE gels (10% Bis-Tris polyacrylamide gels) stained with Coomassie blue dye. The appearance of a band at 14.3 kDa, the size of the Grx protein, was observed.

## Purification of the Grx protein

Cells were broken using an emulsifier (Avestin Emulsiflex C5, Avestin Inc., Ottawa, Canada). After precipitation of nucleic acids by adding 2% (w/v) streptomycin sulfate (SigmaAldrich, USA), the protein solution was dialyzed overnight against 10 mM potassium phosphate pH 6.5 (Sigma-Aldrich, USA), 0.5 mM EDTA (Sigma-Aldrich, USA). After brief centrifugation to remove precipitated protein, the soluble extract was loaded onto a pre-equilibrated SPSepharose HP cation-exchange chromatography column (GE Healthcare, USA). Eluted fractions containing the majority of the Grx protein were identified by SDS-PAGE gels.

Ammonium-sulfate precipitation of protein was performed to concentrate proteins, and the precipitate was recovered by centrifugation. The pellet was resuspended in minimum volume of potassium phosphate/EDTA buffer and then ran through a second column for additional purification. Samples were applied to a Sephadex G50 column (GE Healthcare, USA) equilibrated with 25 mM potassium phosphate pH 7.0, 1mM EDTA, 100 mM NaCl. After analyzing the $A_{280}$ profile for the total protein of the column fractions, a select number of fractions were collected for purity analysis via gel electrophoresis. These fractions were again run on 10% Bis-Tris gels to determine if the Grx protein was expressed, by observing the presence of a band at 14.3 kDa, the proteins known size.

## Kinetic assays

PrxQ thiol reactivity can be measured by an assay in which PrxQ proteins are reacted with Ellman's Reagent, 5,5'-dithiobis (2- nitrobenzoic acid) (DTNB) and observed by absorbance spectrophotometer (Scinco S-3150 UV-Vis Spectrophotometer, Seoul). When DTNB reacts with a thiol, it releases TNB which has a characteristic signal at 412 nm (Figure 4). DTNB also allows for the reaction to be visually tracked because the released TNB causes the solution to turn yellow (Figure 4). To verify the role of each Cys residue in the PrxQ protein, the reaction rates of PrxQ mutants (C48S and C84S) with DTNB were measured using a spectrophotometer which measures absorbance at 412nm. A stock reagent solution of 100mM DTNB was used for the reactions by dissolving 20 mg of DTNB in 0.5 mL of dimethyl sulfoxide (DMSO) (Sigma-Aldrich, USA). In preparation to run the PrxQ C48S and DTNB reaction, 300 µL PrxQ was diluted to 12 mL using 50 mM KPi, 1mM EDTA buffer (pH 7). DTNB solutions were diluted with DMSO, and a total of six concentrations of DTNB were tested: 7µM, 14µM, 21µM, 28µM, 35µM, and 50 µM. 5µL of DTNB solutions were added to the cuvette of 700 µL of the PrxQ C48S solution and reactions were recorded. The spectrophotometer recorded for 300 seconds to cover the entire reaction. This reaction was repeated two times for each concentration of DTNB. The rate of each reaction was recorded by the spectrophotometer and plots of rate versus concentration of DTNB were made using KaleidaGraph (Synergy Software, USA). In PrxQ proteins, two cysteine residues, C48 and C84, are involved in their catalysis reaction. PrxQ C84S only has the peroxidatic cysteine C48 present (C84, the resolving cysteine, is replaced by a serine), so it is prevented from oxidation and forming a disulfide bond with other mutant Cys residues by dithiothreitol treatment (DTT). The peroxidatic cysteine forms the disulfide bond with NTB much faster than the C48S mutant forms a disulfide bond with NTB, so using the absorbance spectrophotometer was insufficient; the reaction was too rapid to be recorded by the spectrophotometer. For this reason, the reactions with the C84S mutant were measured using a stopped-flow spectrophotometer (SX20 Stopped-Flow Spectrometer, Aimil, UK). This technique involves storing the two protein reactants

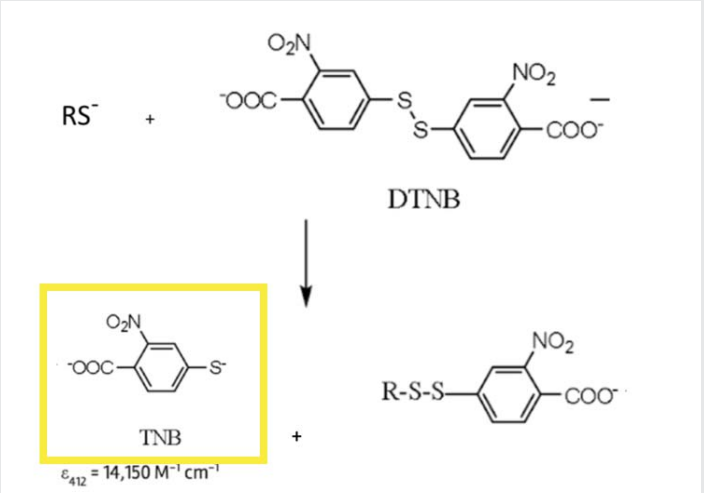


**Figure 4:** Reaction scheme of protein thiol groups with DTNB. This shows the formation of the bound TNB (NTB) to the PrxQ, and the release of TNB. The thiol reduces the disulfide bond and forms its own covalent linkage with DTNB. The free NTB molecule exhibits absorbance at 412nm and produces a yellow color in the solution.



**Citation:** Kreinces J (2020) Identifying potential regulatory interactions of peroxiredoxin PRXQ. Arch Biochem 2(1): 010-019. DOI: https://dx.doi.org/10.17352/ab.000003

in separate reservoirs that are prevented from mixing and depressing the syringes forces the two reactants into a mixing 9 chamber. The reaction is monitored by observing the change in absorbance of the reaction solution. The same reaction conditions as the PrxQ C48S analysis were used.

### Formation of PrxQ-NTB conjugates

Reductant and PrxQ pairs were explored to see which combinations form disulfide bonds that can be used to map catalytically competent electron transfer pathways. NTB-conjugates at single Cys mutants of PrxQ, as mimics of the native disulfide substrates, were used for this analysis.

The protein mutants were reacted with DTNB to form PrxQ C48S-NTB and PrxQ C84S-NTB complexes, to test the reactivity and functionality with Trxs and Grxs. After reacting with DTNB, the Cys residues form disulfide bonds with TNB, which mimics the disulfide form of Prxs after they reduce peroxide. The protein solution was reacted with the 100µM DTNB for 30 minutes, during which the Cys residues reduce the DTNB disulfide, forming a new disulfide with NTB, resulting in the PrxQ-NTB conjugate. The protein complexes were then concentrated using centrifuge ultrafiltration.

### PrxQ-NTB and Trx reduction reactions

The reactions of PrxQ C48S-NTB and PrxQ C84S-NTB with Trx C36S and Trx C33S were observed using visible absorbance spectrophotometry (Scinco S-3150 UV-Vis Spectrophotometer, Seoul). The total 700 µL reaction in the cuvette consisted of 600 µL of PrxQ-NTB complex and 100 µL of KPi/EDTA buffer containing Trx, at varying concentrations of Trx by manipulating the volumes of buffer and Trx. Trx and buffer solutions were added to the PrxQ-NTB complexes in the cuvette. For lower concentrations of Trx, reactions were recorded for 600 seconds while higher concentrations of Trx were recorded for 300 seconds.

### Complex formation analysis of PrxQ-NTB and Trx proteins

Potential PrxQ-Trx complexes were loaded onto Superdex 75 size-exclusion chromatography columns (GE Healthcare, USA) to isolate complexes from other monomeric proteins. Gel electrophoresis with a non-reducing 10% Bis-Tris gels was used to visualize formation of complexes between Trx and PrxQ proteins. To determine if the complexes were formed, the appearance of a band at a molecular weight around 31 kDa, which would represent the summation of the two individual protein's molecular weights (PrxQ, 19 kDa, and Trx, 12 kDa), was searched for.

### PrxQ-NTB and Grx reduction reactions

The reactions of PrxQ C48S-NTB and PrxQ C84S-NTB with Grx C27S and Grx C24S were analyzed by non-reducing gel electrophoresis to determine if PrxQ-Grx complexes formed through disulfide linkage. Small scale reactions consisting of a 2:1 ratio of Grx mutants with PrxQ-NTB complexes were performed. PD10 column filtration (GE Healthcare, USA) was used to remove excess DTT before reacting Grx with DTNB, because it is used to maintain the Grx proteins in their reduced form during storage. DTT treatment of Grx C27S was also necessary as this mutant readily forms a disulfide-linked dimer, thus blocking any reaction with the PrxQ conjugate.

### Complex formation analysis of PrxQ-NTB and Grx proteins

Superdex 75 size-exclusion column chromatography (GE Healthcare, USA) was used to analyze and purify PrxQ-Grx complexes, followed by gel electrophoresis with a non-reducing 10% bis-tris gel to determine if complexes were formed. To analyze complex formation, the appearance of a band at a molecular weight around 31 kDa, which would represent the summation of the two individual protein's molecular weights (PrxQ, 17 kDa, and Grx, 14.3 kDa), was searched for.

### Statistical analysis

In the Trx analysis, varying concentrations of Trx mutants were mixed with 600 $\mu L$ of 1000$\mu$ *M PrxQ-NTB.* Total reactions consisted of 700 $\mu L$ in a cuvette and analyze via absorbance spectrophotometry. A significant more amount of TNB was released from the PrxQ when the PrxQ-NTB conjugate was reacted with the Trx C36S mutant compared to Trx C33S as seen by the higher measured absorbance at 412nm. Data are shown as the mean from two reactions at each concentration of PrxQ-NTB, as seen in Table 1 in the results. T-tests were performed on the means of each reactions using Microsoft Excel (Version 16.44). $P<0.05$ was considered significant.

**Table 1:** Absorbance readings of TNB production as a result of PrxQ C48S-NTB and Trx reactions.

| | | $A_{412}$ (TNB) |
|---|---|---|
| [Trx] (µM) | Trx C36S + PrxQ -NTB | Trx C33S PrxQ-NTB |
| 27 | 0.0731* | 0.0058 |
| 55 | 0.0901* | 0.0056 |
| 82 | 0.0894* | 0.0049 |
| 110 | 0.0841* | 0.0063 |

## Results

### Verification of cloning of the grx gene into the pET28a vector

The first step of this project was to clone the *grx* gene into an expression vector. The company GenScript provided the genes of the Grx mutants to be ligated into the vector. Grx mutant genes were cloned into both expression vectors as BsaI (ends compatible with NcoI) - HindIII fragments (Figure 5). The EcoRV restriction enzyme was used for confirming the inserts were present, as the BsaI/NcoI ligation did not recreate the vector's NcoI site (Figure 6).

Expression from the pET28a vector was much higher than from pTHCΔP (Figure 7). In the gel that confirms successful cloning, lane 10 represents the source of the vector fragment



Citation: Kreinces J (2020) Identifying potential regulatory interactions of peroxiredoxin PRXQ. Arch Biochem 2(1): 010-019. DOI: https://dx.doi.org/10.17352/ab.000003

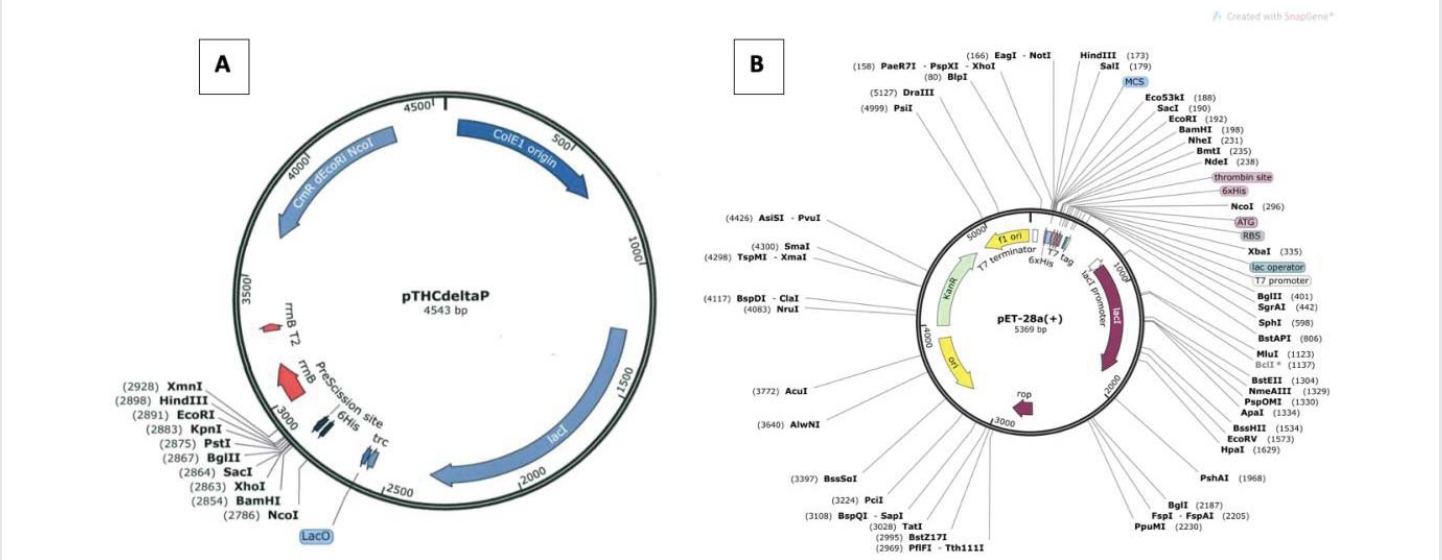


**Figure 5:** Restriction maps of the two vectors used to express the Grx protein gene. A) The restriction map of pTHCdeltaP vector that was used in this study to express the *Xanthononas campestris* Grx protein. B) The restriction map of the pET-28a vector that was used in this study to successfully express the *Xanthononas campestris* Grx protein.

ran as a control to make sure Grx insert was different from Trx insert (Figure 6). The lab had Grx synthesized so the exact size was known to be 350 bp (Figure 6).

## Expression and purification of Grx proteins

The plasmid described above was transformed into competent cells of the BL21 Gold DE3 strain of *E.* coli (Figure 6). The *E. coli* cells containing this plasmid were grown in autoinduction media, which uses lactose as the inducer to synthesize T7 RNA polymerase, which recognizes the T7 promoter of the pET-28a. The T7 promoter is followed by the Grx gene, whose expression is thus induced (Figure 7). Cells were grown at three different temperatures, 16°C, 25°C, and 37°C to determine the temperature to get the best yield of the protein (Figure 7). Small, diluted amounts of each cell lysate were run on the gel. The cell solutions of each expression vector, pET-28a and pTHCΔP, were both run on the gel. Lanes labeled by the numbers 3 and 8 represent the pET-28a transformed cells and the lanes labeled by letters A and F represent the pTHCΔP transformed cells. There was little to no Grx expression in the cells transformed with the pTHCΔP vector, as seen by the lack of Coomassie staining at 14.3 kDa, the known size of Grx. Cells from the 25°C transformed with the pET-28a vector were used, as they yielded the best sample, as judged by the greater Coomassie staining at 14.3 kDa.

For medium-scale purification of Grx mutants, the harvested cell extracts from the 25°C samples were applied to a SP-Sepharose cation-exchange column. The fractions with the highest total protein content based on their $A_{280}$ profiles were subjected to electrophoresis. Fractions 26-37 contained the Grx C27S mutant protein as seen by the bands at 14.3 kDa (Figure 8). These fractions were pooled for further purification and concentrated by precipitation with 30% ammoniumsulfate. The precipitate was recovered by centrifugation, resuspended, and dialyzed overnight against KPi/EDTA buffer (pH 7).

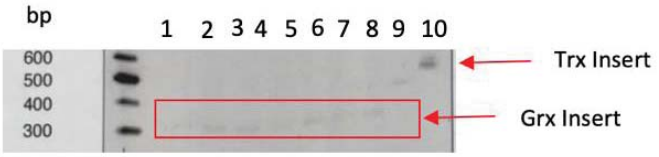


**Figure 6:** Gel confirming the ligation of the Grx gene into the pET28a vector. The faint bands arXcGrx DNA bandound 3 and indicate the correct fragments were made50 bp in lanes 1-8 represent the Nco I and Hind III digested and integrated into the vector. Lane 9 and 10 serve as the control groups to show that the Trx insert into the same expression vector is different than the Grx insert.

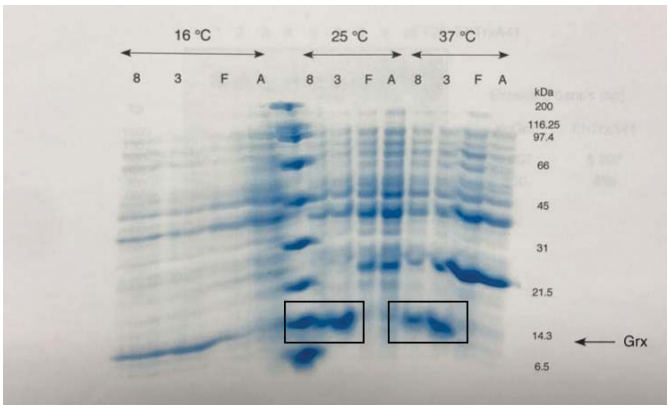


**Figure 7:** *Expression trial of the Grx protein in E. coli* strain BL21 Gold DE3. Cells were grown in auto-induction media to induce the expression of the Grx gene. The numbers 8 and 3 represent that C24S and C27S mutants, respectively, in the pET-28a vector, and the letters F and A represent the C24S and C27S mutants, respectively, ligated into the *pTHCΔP expression vector.* The black rectangles highlight the Grx proteins.

The dialyzed sample was then run over a Sephadex G50 column and fractions run on an SDS-PAGE gel (Figure 9). The purity improved greatly, shown by distinct bands present in the pooled fractions on the SDS-PAGE gel without any other



**Citation:** Kreinces J (2020) Identifying potential regulatory interactions of peroxiredoxin PRXQ. Arch Biochem 2(1): 010-019. DOI: https://dx.doi.org/10.17352/ab.000003

protein present (Figure 9A). For Grx C27S fractions 32 to 41 were collected, and for Grx C24S, fractions 50 to 70 were collected following the final Sephadex G50 column (Figure 9B). Grx C27S elutes in earlier fractions as it more readily forms disulfide bonds with other proteins, thus making it a larger complex to elute sooner in the gel filtration column. The yields of the protein preps were 256 mg of C24S Grx and 69 mg of C27S Grx, both from 2.4 L of auto-induction cultures.

## Trx as a reductant of the PrxQ disulfide bond

Trx C33S and Trx C36S were the two mutants used in this study to determine the reactivity of each Cys residue in forming a complex as a potential reductant with PrxQ. PrxQNTB complexes, which represent the PrxQ in its oxidized form, were reacted with both of these mutants and analyzed via absorbance spectrophotometry and gel electrophoresis. These two Trx proteins were analyzed as potential reductants of the PrxQ protein disulfide to return the PrxQ to a catalytically active state. The Trx mutants (lacking one of the Cys residues) rather than wild type Trx were used so that, once formed, the disulfide bond between the PrxQ and Trx proteins would be stabilized. Once the PrxQ-NTB conjugates were generated, they were reacted with the Trx or Grx proteins to determine if either of these reducing proteins would bind to the PrxQ, representing a potential electron transfer interaction.

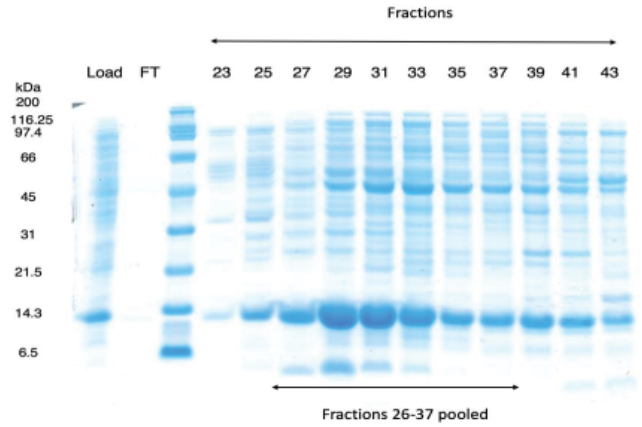


**Figure 8:** Initial purification results. Resulting gel from the SP-sepharose cation-exchange column of Grx C27S. Fractions 26-37 were pooled for further purification and precipitation.

Trx C36S was the only Trx that indicated any interaction with the PrxQ C48S-NTB complex, as evidenced by the band at a molecular weight around 31 kDa (Figure 10). When PrxQ C48S-NTB was mixed with Trx C33S, no reaction took place. The formation of a complex between PrxQ and Trx C36S and the lack of complex formation between PrxQ and Trx C33S is also evidenced by the amount of free TNB released from the reaction (Table 1). Released TNB signifies the Trx reduced the PrxQ-NTB disulfide bond. When PrxQ was reacted with Trx C36S, significantly more TNB was released into solution (Figure 10). The PrxQ C84S-NTB complex did not react at all with either the Trx C36S or Trx C33S, as evident by zero absorbance change at 412 nm observed on the spectrophotometer. PrxQ C84S-NTB was also reacted with both Trx mutants in test tubes overnight to determine if the reaction occurred at all, but showed no signs of reactions, as there was no color change produced by cleavage of free TNB. Based on the absorbance spectrophotometer results, PrxQ C48S-NTB and Trx C36S served as a positive control, and produced a yellow solution in the test tubes, confirming that PrxQ C48S-NTB and Trx C36S yielded the only evident reaction.

## Chromatographic and SDS-PAGE analysis of PrxQ and Trx Covalent linkage formation

Assessing the PrxQ C48S and Trx C36S reaction for the formation of a complex, the gel column shows that the PrxQ C48S-TNB and Trx C36S reacted and formed a complex as expected at 31,000 Da, which is indicated by the large protein

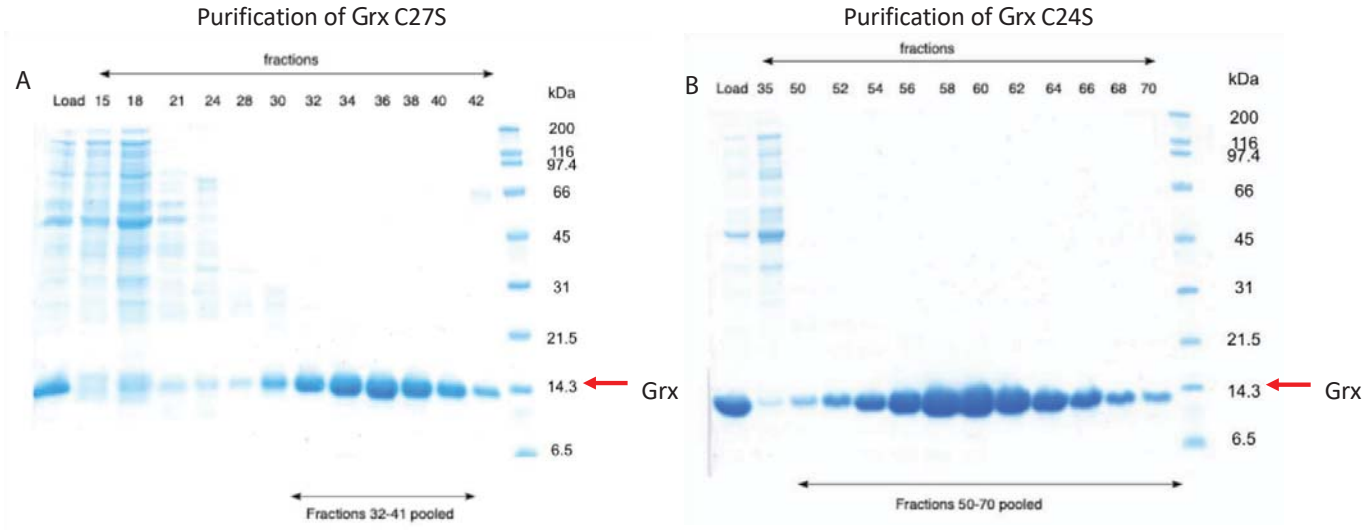


**Figure 9:** Final purification results. **A)** Resulting gel from the purification of the Grx C27S mutant following gel filtration chromatography. The fractions 32-collected as it is clear that the Grx protein around 14 kDa (red arrow) is the sole protein present in these samples, indicating a pure solution. **B)** Resulting gel from the purification of the Grx C24S mutant following anion-exchange chromatography, Fractions 50-70 were collected. These are the purest samples around the weight of Grx at 14 kDa, as indicated by the red arrow. Coomassie blue staining was used to visualize the protein. Sephadex G50 columns were used for both mutants.



**Citation:** Kreinces J (2020) Identifying potential regulatory interactions of peroxiredoxin PRXQ. Arch Biochem 2(1): 010-019. DOI: https://dx.doi.org/10.17352/ab.000003

marking on the resulting gel (Figure 10). This is about the correct spot we would expect to see that complex, as it represents the additive molecular weights of PrxQ and Trx proteins. PrxQ and Trx are able to form a covalent link as the Prx protein is missing its other Cys residue. Such complexes mimic the intermediates formed during electron transfer, and therefore would provide structural information about molecular interactions if analyzed by crystallography. However, X-ray crystallographers could not form crystals of the PrxQ/Trx C36S material that we sent to them.

## Grx possibly reducing the PrxQ disulfide bond

Similar to the Trx mutant reactions with PrxQ, two Grx mutants (C24S and C27S) were analyzed as potential reductants of the PrxQ protein. Unlike the Trx trials, the kinetics of the Grx reactions with PrxQ-NTB have not yet been measured, as the only objective at this stage was to form complexes between the two that we could analyze for potential reduction interactions. PrxQ-NTB complexes were reacted with two different amounts (15 $\mu$L and 5 $\mu$L) of Grx protein for each mutant. The reaction solutions were then analyzed via gel electrophoresis, in which the gels indicate several spurious complexes formed (Figure 9). As indicated by the larger band around 31 kDa, more complex formed between PrxQ-NTB and Grx C27S, although it is a partial complex formation, as seen by the many other bands present. In the complex reaction lanes, there is still a clear appearance of the PrxQ monomer around 18 kDa, Grx monomers around 10 kDa, and Grx dimers directly under the complex around 25 kDa (Figure 11). These Grx dimers are present in the Grx control lane and would carry over to appear in the complex reactions as the dimers' thiol group is oxidized in a disulfide bond, making it unreactive. It is possible that upon DTT removal, the cysteines were oxidized by air which allowed them to form the disulfide bond or that there are other side chains involved preventing a clean bonding interaction. None of these complexes were selected for further analysis through X-ray crystallography, as we wanted to obtain a purer sample first.

The reactions between Grx mutants and PrxQ-NTB were then repeated with Tris buffer of pH 8 hoping it may make the thiolate ion on the cysteines more reactive and help for a purer complex. The higher pH would make ensure the hydrogen would be removed from the thiol group, and thus forming the reactive thiolate ion which could potentially attack the PrxQ-NTB disulfide bond. Grx mutants and PrxQ-NTB were reacted in a 2:1 ratio, as it is easier to remove excess Grx through column chromatography than the larger PrxQ-NTB complex. Again, spurious complexes were identified via gel electrophoresis, however, more complex was formed with the Grx C27S mutant rather than the C24S mutant (Figure 12). Grx monomers and dimers are again present on the gel in the control group and complex forming group, which explains the large band below the complex around 31 kDa (dimer), and the band around 14 kDa (monomer).

## Kinetics of PrxQ C48S and C84S reactions with DTNB

The reaction of each mutant of PrxQ with DTNB was analyzed to determine the reactivity of each cysteine residue.

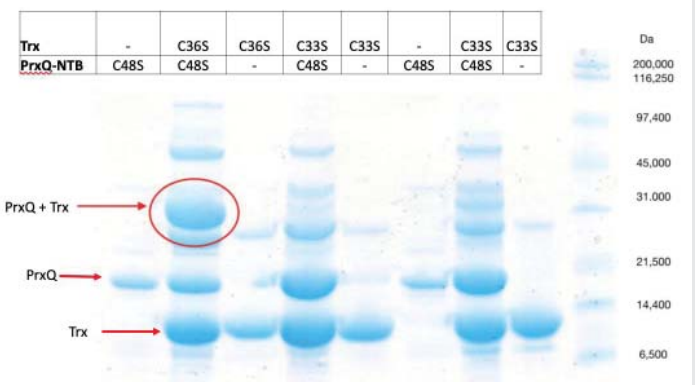


**Figure 10:** *Non-reducing gel column displaying the PrxQ-NTB reactions with Trx C36S and Trx C33S.* This shows that the PrxQ C48S-NTB and Trx C36S reaction formed the expected protein complex at 31,000 Da, indicated by the large band circled in red. The two proteins, PrxQ at 14,300 Da and the Trx protein at 10,000 Da, make up the complex which is why we see the band at the larger weight. This solution was sent to be crystallized.

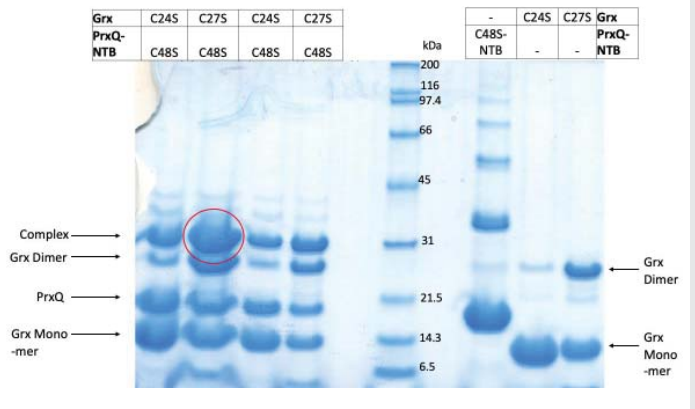


**Figure 11:** Complex formation analysis via gel electrophoresis. The lanes to the left of the standard protein ladder represent the PrxQ C48S and Grx complexes, at varying amat higher Grx concentrations (15 $\mu L$) as compared to duplicated expierents adjacent to those lanes (5ounts of Grx mutant. The two most left lanes were ran L).The red oval is used to show that more complex was formed between PrxQ C48S and Grx C27S than with Grx C24S.

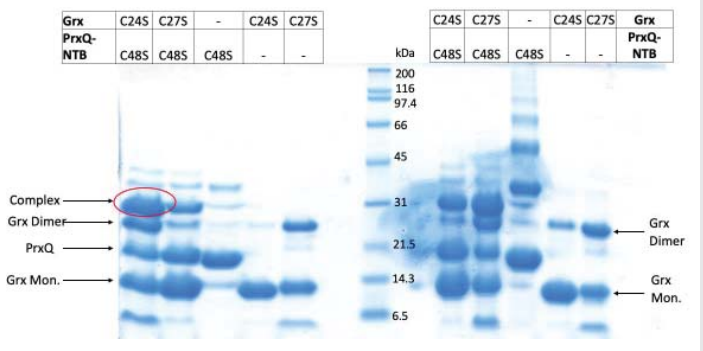


**Figure 12:** Complex formation analysis via gel electrophoresis after Tris buffer treatment. The lanes to the right of the standard protein ladder represent the proteins and complex solutions when treated with the Kpi/EDTA pH 7 buffer, as seen in Figure 8. The lanes to the left of the standard protein ladder represent the proteins and complex solutions when treated with Tris buffer pH 8 in attempting to increase the reactivity of the thiolate ions. The red circle on the left is there to show that the PrxQ C48S-NTB conjugate formed more complex with the Grx C24S mutant in this trial. The unmarked bands below the Grx monomer around 6.5 kDa are degraded protein products.



**Citation:** Kreinces J (2020) Identifying potential regulatory interactions of peroxiredoxin PRXQ. Arch Biochem 2(1): 010-019. DOI: https://dx.doi.org/10.17352/ab.000003

The rate of the reaction with protein increased with higher concentrations of DTNB. This allows us to characterize the enzyme-DTNB reaction as second order, as the rate increases in a dose-dependent manner with DTNB treatment. For the C48S reactions, the average rate constant was 21.4 $M^{-1}$ $s^{-1}$, and for the C84S reactions, the average rate was 25700 $M^{-1}$ $s^{-1}$. This supports the previous study that Cys 48 is the reactive, peroxidatic Cys, as the mutant with only the peroxidatic residue remaining (C84S) reacted with the disulfide of DTNB much faster [8]. Duplicates of each reactions were performed to confirm that these second order reactions are reproducible (Figure 13).

## Discussion

Prxs are ubiquitous peroxidase enzymes that have emerged as some of the most important proteins involved in regulating hydrogen peroxide levels. They play crucial roles in defending cells against oxidative stress, in redox regulatory pathways, and as pathogenic factors in diseasecausing organisms. The study by Perkins et al. that preceded this paper produced ultra-highresolution structures of *Xc*PrxQ at about 1.0 Å [8]. These structures obtained during Prx reactions reveal a high level of detail about active site interactions throughout the Prx catalysis mechanism, representing a strong starting point for further studies on this protein [8].

In this study, potential cysteine residues of Trx and Grx proteins are identified that could serve to react with the PrxQ disulfide and reduce it back to a catalytically active form. Trx and Grx were selected for their well-studied mechanism in redox catalysis and molecular signaling in many organisms, as well as for their potential health significance [11-14].

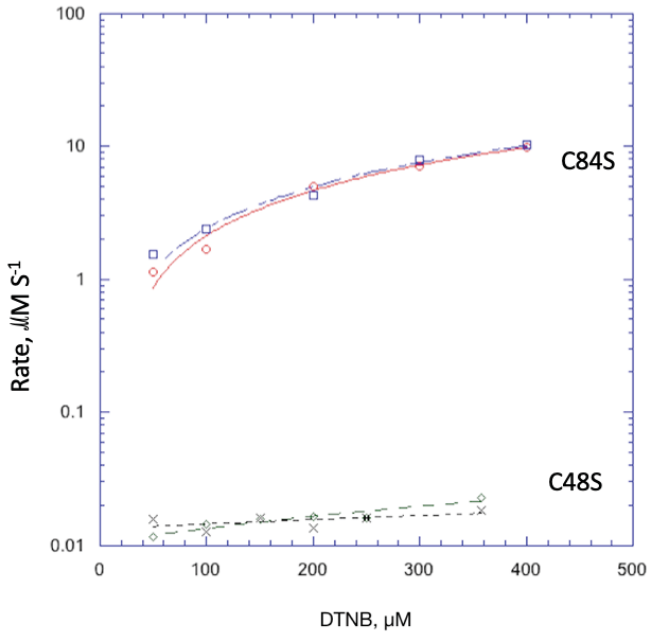


**Figure 13:** Kinetic analysis of PrxQ mutant reactions with DTNB. The back and green curve fit lines represent the rate constants of the two trials of the reactions between PrxQ C48S and DTNB. The red and blue curve fit lines represent the rate constants of the two trials of the reactions between PrxQ C84S and DTNB. The graph indicates that the reactions are reproducible for both mutants.

When reacting the PrxQNTB complexes with the two mutated Trxs, only the PrxQ C48S-NTB complex yielded a measurable reaction. As PrxQ C48S is the mutant with the missing reactive cysteine (peroxidatic cysteine), this indicates that the resolving cysteine (which this mutant still has) is accessible to the Trx reductant. However, this mutant only reacted with Trx C36S, suggesting the Cys 33 residue is more reactive than the Cys 36 residue in Trx, as Cys 33 in the Trx C36S mutant successfully attacked the disulfide bonds. This is suggesting that Cys 33 is the reactive cysteine in the wild type Trx protein in *X. campestris*. None of the reactions of PrxQ C84S-NTB showed any measurable rate, which could mean that the reactive Cys is not accessible due to the protein conformation.

To determine if PrxQ-NTB and Trx formed a covalent linkage as a potential interaction, we reacted the two proteins and analyzed the reactions via light absorbance spectrophotometry and gel electrophoresis. The analysis of the complexes as seen in the gel images in Figures 10-12 shows that the complexes are variable in content. This may occur because single cysteines on PrxQs are coming together to give the disulfide bonded dimer. It is possible that this dimer was artifactually formed at the time of gel preparation in the absence of an alkylating agent. Boiling the samples before running the gel may have allowed the free thiols to form a disulfide bond. The same reaction could happen with the Trxs, giving a Trx dimer and PrxQ dimer, which is not what would be seen *in vivo* in the wild type forms of the protein [8]. PrxQ is known to be 19 kDa so the dimer is the faint band seen around 38 kDa in Figure 7, making it inaccessible to the Trx for reduction. In the complex solution lane in Figure 8, many protein bands were found including the PrxQ-Trx covalent linkage. PrxQ dimers are present under the PrxQ-Trx complex, while there are larger sized proteins also present which could be another protein from the bacteria (Figure 10).

The PrxQ-NTB and Grx complexes analyzed via gel electrophoresis show the presence of Grx dimers and monomers (Figures 11,12). The proper complex is seen right above the Grx dimer, which is present when Grx is reacted with PrxQ-NTB because the Grx dimer is unreactive as the cysteines are in a disulfide bond and are inaccessible to react; the dimer can no longer react because it doesn't have a free thiol. A potential explanation for the appearance of the Grx dimer and the spurious complex is that both Grx mutants are treated with a large amount of DTT to prevent disulfide formation between monomer subunits. As soon as the DTT is removed through the PD10 column, the protein's cysteines may become air oxidized, which could explain the formation of the dimer through disulfide linkage. Many of the reactions were not conducted immediately after removal of DTT. To further explore the interaction between PrxQ and Grx, a Y19W mutation could be made in the Grx gene, which will provide a fluorescent signal and allow tracking of the entire reaction and measure the kinetics by stopped-flow analysis, offering a more complete picture of the reaction and potential obstacles.

The immediate goal remains to obtain a complex of PrxQ and Grx that diffracts X-rays. As the structure of PrxQ is now well known, that can be used to help solve the structure



**Citation:** Kreinces J (2020) Identifying potential regulatory interactions of peroxiredoxin PRXQ. Arch Biochem 2(1): 010-019. DOI: https://dx.doi.org/10.17352/ab.000003

of PrxQ/reductant complexes and determine how they specifically interact, including which side chains interact and what important amino acid residues are involved. Analysis of the complex can be done through molecular modeling, which uses computer-based techniques to analyze structures and reactions of molecules. This could allow us to determine how certain interactions contribute to overall structure. Targeted mutations on both Prx and target reductant proteins could be designed to see how certain residues affect enzyme. This could potentially lead to manipulating the structure such as counteracting charges to see if there would be improvement in interactions with the specific Prx protein.

The impact of Prx function on regulating ROS levels and defending the cell against oxidative stress may prove to be crucial in pathological situations such as cancer in which its efficiency is reduced [15]. Increased knowledge of Prx structure and function in addition to the identification of reductant pathways will pave the way for eventually modulating human and pathogen Prx activity in ways that will enhance their function or block pathways that promote pathogenesis. The antioxidant Prxs have attracted the attention of cancer researchers for their apparent function as tumor suppressors, as high Prx levels have been associated with the resistance of tumors and cancer cell lines to immune system defenses [4]. ROS have also been linked to other very prevalent diseases such as atherosclerosis, Alzheimer's disease, and Chronic Obstructive Pulmonary Disease (COPD), highlighting the importance of Prx proteins in providing effective defense against oxidative stress [2]. As key regulators of intracellular hydrogen peroxide levels, developing a further understanding of these proteins and their function can lead to meaningful biological and medicinal advancements.

Hydrogen peroxide can be a beneficial as well as a harmful ROS [2]. It is an important signaling factor in major processes including cell proliferation, differentiation, tissue repair, and inflammation [1,3]. It has also been found to function as a second messenger in insulin signaling, growth-factor signaling, and immune system signaling cascades [13]. At excessively high amounts, hydrogen peroxide can cause damaging oxidation to proteins, nucleic acids, and membrane lipids. Oxidative DNA damage is one of the major contributors to cancer development, as oxidative stress can induce base lesions, DNA cross-links, and strand breaks which can lead to tumor onset [2,16,17].

In multicellular organisms, ROS are also involved in cell proliferation, differentiation, migration, and apoptotic responses, while also regulating the transcription of genes encoding antioxidants at the transcriptional level [18]. For example, the expression of transcription factor p53 directly depends on intracellular peroxide concentration; at low levels of peroxide, p53 drives the expression of genes encoding antioxidants which protect cells from damage while at high peroxide levels, p53 stimulates the expression of pro-oxidants and other factors involved in apoptosis [18]. Thus, as a signaling molecule, ROS can induce a diverse set of biological responses that are crucial for cell health and function. Numerous subtypes of Prxs in mammals have been found to play crucial roles in cell proliferation, differentiation, and immune system function, exemplified by a Prx1 knockout mouse developing many types of cancer before the age of one [19]. A recent study in a human cell line demonstrated that Prx2 is a crucial component in a peroxideredox relay that regulates the transcriptional activity of STAT3, a crucial immune system protein involved in helper T cell differentiation [16,17].

Prxs from human pathogens are also novel targets for antibiotic development, as they are important in oxidative stress defense and other biological processes in these organisms. Given the increasing realization of the importance of Prxs, our long-term goal is understanding the functional and structural determinants of Prx activity and regulation to define and potentially manipulate their biological functions for improving human health. Crystallized complexes between PrxQ and Trx or Grx reductants can serve as models for drug targets in disease causing organisms, as inhibiting these systems can reduce their ability to regulate hydrogen peroxide levels. This study helps progress toward the long-term goal of understanding the functional and structural determinants of Prx activity and regulation with the goal of manipulating human and bacterial Prx regulation for improving human health by increasing the efficiency of the Prx catalytic cycle and inhibiting bacterial Prx function, respectively.

## Conclusion

The reactivity of Trx and Grx mutants with disulfide-containing PrxQ variants was assessed using light absorbance spectroscopy and *in-vitro* enzyme assays. Through gel electrophoresis of possible complexes of single Cys mutants of PrxQ and reductants, it was observed that the Trx mutant C36S formed the most identifiable complex with PrxQ C48S, but this has not yet been confirmed by X-ray crystallography. In summary, two potential reductants have been identified which can increase PrxQ efficiency and overall ability of the protein to reduce peroxide and protect against oxidative stress.

## References

1. Sies H (2017) Hydrogen peroxide as a central redox signaling molecule in physiological oxidative stress: Oxidative eustress. Redox Biol 11: 613-619. Link: https://bit.ly/3o47XDa

2. Pizzino G, Irrera N, Cucinotta M, Pallio G, Mannino F, et al. (2017) Oxidative Stress: Harms and Benefits for Human Health. Oxid Med Cell Longev 2017: 8416763. Link: https://bit.ly/3bWMidZ

3. Sies H (2014) Role of metabolic H2O2 generation: redox signaling and oxidative stress. J Biol Chem 289: 8735-8741. Link: https://bit.ly/3iv7UPM

4. Ghosh N, Das A, Chaffee S, Roy S, Sen CK (2018) Chapter 4 - Reactive Oxygen Species, Oxidative Damage and Cell Death. In: Chatterjee S, Jungraithmayr W, Bagchi D, eds. Immunity and Inflammation in Health and Disease. Academic Press 45-55. Link: https://bit.ly/3o55ZT4

5. Perkins A, Nelson KJ, Parsonage D, Poole LB, Karplus PA (2015) Peroxiredoxins: guardians against oxidative stress and modulators of peroxide signaling. Trends Biochem Sci 40: 435-445. Link: https://bit.ly/392QUNS

6. Dubbs JM, Mongkolsuk S (2007) Peroxiredoxins in bacterial antioxidant defense. Subcell Biochem 44: 143-193. Link: https://bit.ly/392pDek



Citation: Kreinces J (2020) Identifying potential regulatory interactions of peroxiredoxin PRXQ. Arch Biochem 2(1): 010-019. DOI: https://dx.doi.org/10.17352/ab.000003

7. Kaihami GH, Almeida JR, Santos SS, Netto LE, Almeida SR, et al. (2014) Involvement of a 1-Cys peroxiredoxin in bacterial virulence. PLoS Pathog 10: e1004442. Link: https://bit.ly/35W6Y1F

8. Perkins A, Parsonage D, Nelson KJ, Ogba OM, Cheong PH, et al. (2016) Peroxiredoxin Catalysis at Atomic Resolution. Structure 24: 1668-1678. Link: https://bit.ly/3qwvsXo

9. Hall A, Karplus PA, Poole LB (2009) Typical 2-Cys peroxiredoxins--structures, mechanisms and functions. FEBS J 276: 2469-2477. Link: https://bit.ly/2KCM1lc

10. Reeves SA, Parsonage D, Nelson KJ, Poole LB (2011) Kinetic and thermodynamic features reveal that Escherichia coli BCP is an unusually versatile peroxiredoxin. Biochemistry 50: 8970-8981. Link: https://bit.ly/39PJFYz

11. Hanschmann EM, Godoy JR, Berndt C, Hudemann C, Lillig CH (2013) Thioredoxins, glutaredoxins, and peroxiredoxins--molecular mechanisms and health significance: from cofactors to antioxidants to redox signaling. Antioxid Redox Signal 19: 1539-1605. Link: https://bit.ly/3pambEg

12. Ma H, Wang M, Gai Y, Fu H, Zhang B, et al. (2018) Thioredoxin and Glutaredoxin Systems Required for Oxidative Stress Resistance, Fungicide Sensitivity, and Virulence of Alternaria alternata. Appl Environ Microbiol 84: e00086-18. Link: https://bit.ly/3956tEN

13. Haffo L, Lu J, Bykov VJN, Martin SS, Ren X, et al. (2018) Inhibition of the glutaredoxin and thioredoxin systems and ribonucleotide reductase by mutant p53-targeting compound APR-246. Sci Rep 8: 12671. Link: https://bit.ly/3qJtuTH

14. Sengupta R, Holmgren A (2014) Thioredoxin and glutaredoxin-mediated redox regulation of ribonucleotide reductase. World J Biol Chem 5: 68-74. Link: https://bit.ly/390mWKm

15. Aggarwal V, Tuli HS, Varol A, Thakral F, Yerer MB, et al. (2019) Role of Reactive Oxygen Species in Cancer Progression: Molecular Mechanisms and Recent Advancements. Biomolecules 9: 735. Link: https://bit.ly/3o43II7

16. Sobotta MC, Liou W, Stöcker S, Talwar D, Oehler M, et al. (2015) Peroxiredoxin-2 and STAT3 form a redox relay for H2O2 signaling. Nat Chem Biol 11: 64-70. Link: https://bit.ly/2Nj7y37

17. Kang SW, Lee S, Lee JHS (2018) Cancer-Associated Function of 2-Cys Peroxiredoxin Subtypes as a Survival Gatekeeper. Antioxidants (Basel, Switzerland) 7: 161. Link: https://bit.ly/2KxPukS

18. Veal E, Day A (2011) Hydrogen peroxide as a signaling molecule. Antioxid Redox Signal 15: 147-151. Link: https://bit.ly/393u20M

19. Neumann CA, Krause DS, Carman CV, Das S, Dubey DP, et al. (2003) Essential role for the peroxiredoxin Prdx1 in erythrocyte antioxidant defence and tumour suppression. Nature 424: 561-565. Link: https://bit.ly/393cIIZ








**Citation:** Kreinces J (2020) Identifying potential regulatory interactions of peroxiredoxin PRXQ. Arch Biochem 2(1): 010-019. DOI: https://dx.doi.org/10.17352/ab.000003